Supporting Information

Development of Palladium, Gold and Gold-Palladium Containing Metal-Carbon Nanoreactors: Hydrogen Adsorption

Vishal J. Mayani, Suranjana V. Mayani, and Sang Wook Kim*

*Department of Advanced Materials Chemistry, College of Science and Technology, Dongguk University–Gyeongju, Gyeongbuk 780-714, Korea. *E-mail: swkim@dongguk.ac.kr*

Received December 3, 2013, Accepted January 3, 2014

Synthesis of Carbon Gold Palladium (CGPC) Composite Materials. Figure 1 represents the schematic diagram of preparation of two sized (25 and 170 nm) carbon cage (CC), carbon silica composite (CSC), carbon gold composite (CGC), carbon palladium composite (CPC) and carbon gold palladium composite (CGPC) material from low-cost pyrolysis fuel oil (PFO) based pitch.

Preparation of Nano Silica Ball (NSB-25/170). Nano silica ball (NSB) was prepared by hydrolysis and condensation of TEOS. Here, we have synthesized two sets of NSB (25 nm and 170 nm). In a typical synthesis of NSB-25, 10 mL distilled water and 7.8 mL of TEOS were stirred (400 rpm) in 500 mL of absolute ethanol (EtOH) for 30 min. 4 mL of NH_4OH (28 wt %) was added to the resulting mixture, which was left to stir for further 24 h at room temperature at 400 rpm. The reaction mixture was transferred to oven and heated at 70 °C until complete dryness. The solid product was washed (ethanol and warm water) and dried at room temperature in air. The resulted NSB-25 were calcined at 550 °C for 6 h. (NSB-25); yield (2.3 g), BET Surface area of NSB-25: 30 m^2/g, FTIR (KBr) 811, 1104, 1627, 1870, 3439, 3746 cm^{-1}. (NSB-170); yield (6.1 g), FTIR (KBr) 469, 553, 799, 949, 1096, 1396, 1632, 3430 cm^{-1}, BET Surface area of NSB-170: 163 m^2/g.[1]

Synthesis of Carbon Cage (CC-25/170). The CC-25/170 materials were prepared as shown in Figure 1. The pitch residue, used as a CC precursor, was prepared according to the method reported previously under a heat extraction and self-crystallization method.[2] For a typical procedure, 12 g of pitch was heated at 50 °C and mixed homogeneously with 10 g of NSB-25/NSB-170 in crucible for 10 min. After cooling to room temperature, the mixture was carbonized at 900 °C for 4 h under nitrogen atmosphere to produce the carbon silica composite (CSC-25/170) material. The resulting CSC-25/170 material was treated with 10% hydrofluoric acid (HF) for 12 h. The solid carbon cage (CC-25/170) material was washed with distilled water and followed by drying at 100 °C in oven. (CC-25); yield (6.3 g), BET Surface area of CC-25: 82 m^2/g, FTIR (KBr) 1113, 1584, 1620, 3437 cm^{-1}. Elemental analysis results showed that CC-25 contained > 94 wt % carbon and < 1.2 wt % H after carbonization at > 900 °C. (CC-170); yield (6.2 g), BET Surface area of CC-170: 212 m^2/g, FTIR (KBr) 811, 1099, 1257, 1602, 3453 cm^{-1}. Elemental analysis results showed that CC-170 contained > 95 wt % carbon and < 0.4 wt % H after carbonization at > 900 °C.[3]

Synthesis of Carbon Gold Composite (CGC-25/170). In order to prepare the CGC-25/170, 3.07 g of CC-25/170 were added in 250 mL of sodium citrate dihydrate solution and the mixture was then exposed to ultrasonic process for 5 min. The suspension of CC-25/170 was then transferred to 250 mL of distilled water. The diluted suspension was refluxed with stirring for 5 min, followed by the addition of 1% $HAuCl_4$ (100 mL) to the suspension containing CC-25/170. The resulting suspension was stirred at boiling temperature for next 5 min. The resulting solid particles were filtered with a Buchner funnel and washed with distilled water. The powder was dried in air at 100 °C. Finally, the solid was calcined at 900 °C for 1 h in nitrogen to yield CGC-25/170 (Figure 1). (CGC-25); Yield: 3.5 g, BET surface area of CGC-25: 75 m^2/g, FTIR (KBr) 1119, 1254, 1579, 3449 cm^{-1}. Elemental analysis and ICP results showed that CGC-25 contained > 85 wt % carbon and > 11.0 wt % Au after carbonization at > 900 °C. (CG**C**-170); Yield: 3.6 g, BET surface area of CGC-170: 184 m^2/g, FTIR (KBr) 806, 1116, 1590, 3487 cm^{-1}. Elemental analysis and ICP results showed that CGC-170 contained > 86 wt % carbon and > 10.2 wt % Au after carbonization at > 900 °C.[3]

Synthesis of Carbon Palladium Composite (CPC-25/

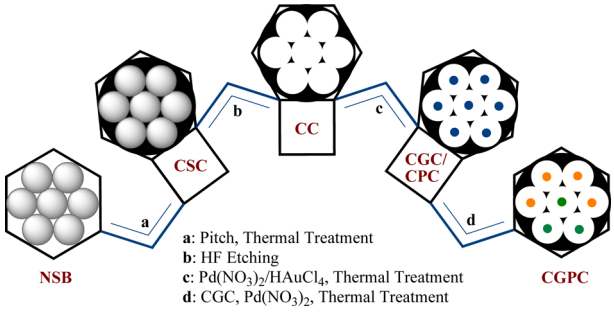

Figure 1. Schematic illustration for the synthesis of CGC, CPC and CGPC.

170). Typically, take 3 g of CC-25/170 in 100 mL of distilled water and add 100 mL (0.5 wt %) palladium nitrate dehydrate ($Pd(NO_3)_2{\cdot}2H_2O$) solution and sonicate it for 1 h. Then mixture was heated for 3 h at boiling temperature. 2% sodium borohydride ($NaBH_4$) solution (in water) was added dropwise (50 mL). The mixture was dried in air at 110 °C. Then mixture was activated at 800 °C for 30 min in tubular furnace in presence of argon gas. After activation, the carbon was cooled to room temperature in a flow of argon. To remove the excess salt, the samples were extensively washed with hot water in Soxhlet extractor until the pH of the washing become neutral. Then sample were dried in oven at 110 °C. (CPC-25); Yield: 3.2 g, BET surface area of CPC-25: 66 m^2/g, FTIR (KBr) 1131, 1233, 1569, 3434 cm^{-1}. Elemental analysis and ICP results showed that CPC-25 contained > 91 wt % carbon and > 2.3 wt % Pd after carbonization at > 900 °C. (CPC-170); Yield: 3.3 g, BET surface area of CPC-170: 178 m^2/g, FTIR (KBr) 1271, 1546, 1581, 2343, 3441 cm^{-1}. Elemental analysis and ICP results showed that CPC-170 contained > 90 wt % carbon and >3.4 wt % Pd after carbonization at > 900 °C.

Synthesis of Carbon Gold Palladium Composite (CGPC-25/170). In the mixture of distilled water (100 mL) and 3 g of CGC-25/170, add 100 mL of 0.5 wt % palladium nitrate dehydrate ($Pd(NO_3)_2{\cdot}2H_2O$) solution and sonicate it for 1 h. Process was followed by heating for 3 h at boiling temperature. 2% sodium borohydride ($NaBH_4$) aqueous solution was added dropwise (50 mL). The mixture was dried in air at 110 °C and further activated at 800 °C for 30 min in tubular furnace through argon gas purging. Later, the resultant carbon was cooled to room temperature in a flow of argon. In order to remove excess salt, the samples were continuously treated with hot water in Soxhlet extractor until the pH of the washing become neutral. Then sample were dried in oven at 110 °C. (CGP**C**-25); Yield: 3.1 g, BET surface area of CGPC-25: 63 m^2/g, FTIR (KBr) 1237, 1577, 3433 cm^{-1}. Elemental analysis and ICP results showed that CGPC-25 contained > 80 wt % carbon, > 9.1 wt % Au and > 6.8 wt % Pd after carbonization at > 900 °C. (CGP**C**-170); Yield: 3.2 g, BET surface area of CGPC-170: 218 m^2/g, FTIR (KBr) 1580, 1655, 3436 cm^{-1}. Elemental analysis and ICP results showed that CGPC-170 contained > 82 wt % carbon, > 4.5 wt % Au and > 2.9 wt % Pd after carbonization at > 900 °C.

Materials, Characterization and Analysis. Pyrolysis fuel oil (PFO) was obtained from YNCC (Yeocheon Naphtha Cracking Center, Korea). Other chemicals such as ethanol, toluene, sulfuric acid, sodium hydroxide, ammonium hydroxide, sodium citrate dihydrate (Dae-Jung Chemicals & Metals Co. Ltd., Korea), tetraethylorthosilicate (TEOS), Palladium nitrate dehydrate ($Pd(NO_3)_2{\cdot}2H_2O$), sodium borohydride ($NaBH_4$) (Aldrich, USA), hydrofluoric acid (J. T. Baker, USA) and hydrogen tetrachloroaurate (III) hydrate ($HAucl_4$) (Kojima Chemicals Co. Ltd, Japan) were used as received. All the solvents were purified by known method.[4]

The different sized (25 and 170 nm) composite carbon materials CC, CGC, CPC and CGPC were characterized by powder X-ray diffraction (PXRD, Phillips X'pert MPD diffractometer, Almelo, The Netherlands) in 2θ range (10–80) at scan step 0.02°. Fourier transform Infrared spectroscopy were completed (FTIR Perkin-Elmer Spectrometer, Massachusetts, USA) using KBr self supported pellet technique. Microanalysis of the products was carried out by a CHN analyzer (CE instruments, UK) and the metals entering into the carbon cage was determined with inductively coupled plasma-optical emission spectroscopy (ICP-OES, JY Ultima 2CHR). BET surface area was determined by N_2-sorption data measured at 77 K using volumetric adsorption set up (Micromeritics ASAP-2010, USA). The pore diameter of the samples was determined from the desorption branch of nitrogen adsorption isotherm employing the Barret-Joyner-Halenda (BJH) model. Thermal measurements and microstructure evaluation of these samples were carried out on thermo-gravimetric analyzer (TGA, SDT600, TA instrument, USA) and scanning electron microscopy coupled with energy dispersive spectroscopy (SEM-EDS, LEO-1430, VP, UK), transmission electron microscopy (TEM, JEM 2011, Jeol Corporation, Japan). The hydrogen adsorption isotherms were performed by using gravimetric measurement with a Rubotherm MSB in four steps: blank measurement, loading and reactivation of samples, buoyancy measurement and adsorption measurement.

Characterization. The synthesized palladium, gold and gold-palladium incorporated carbon nanocomposites were fully characterized by microanalysis, N_2 adsorption–desorption isotherm, SEM–EDS, TEM, ICP, TGA, PXRD and FTIR (See Figures 2 to 17).

Characterization by Powder X-ray Diffractions. Low-angle and wide-angle powder X-ray diffractions (PXRD) were used to characterize the all MCNRs. Low-angle PXRD (1–10°) measurement did not produce any characteristic peak which indicates short range order or disordered phases present in the all MCNRs prepared (Figures 2-3).

The wide-angle PXRD profile of NSB-25 showed (Figure 4) one broad peak assigned at 2θ = 23.3°, corresponding to

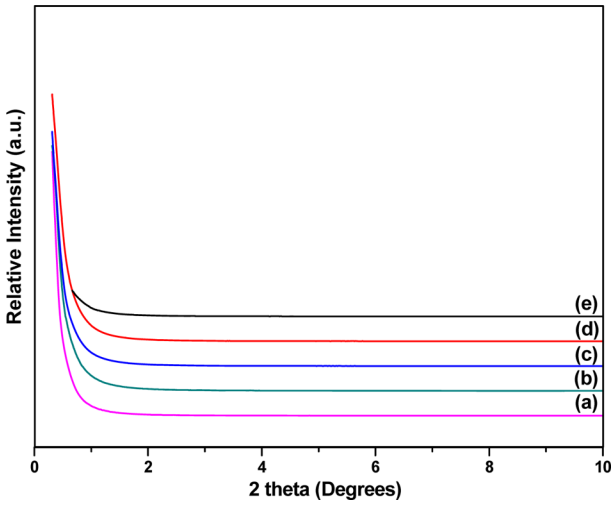

Figure 2. Low-angle PXRD patterns of NSB-25 (a), CC-25 (b), CGC-25 (c), CPC-25 (d) and CGPC-25 (e).

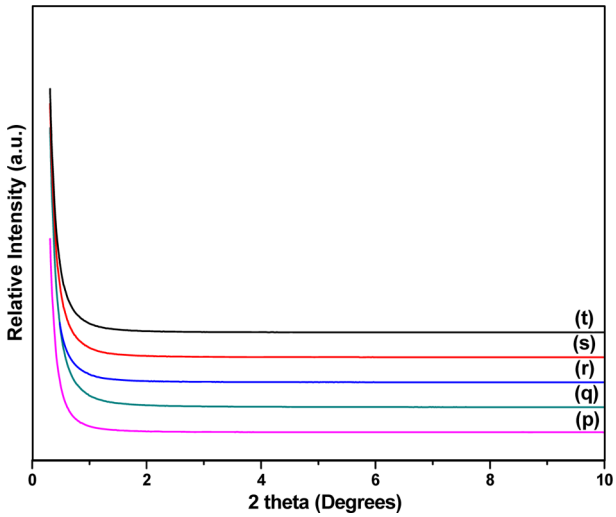

Figure 3. Low-angle PXRD patterns of NSB-170 (p), CC-170 (q), CGC-170 (r), CPC-170 (s) and CGPC-170 (t).

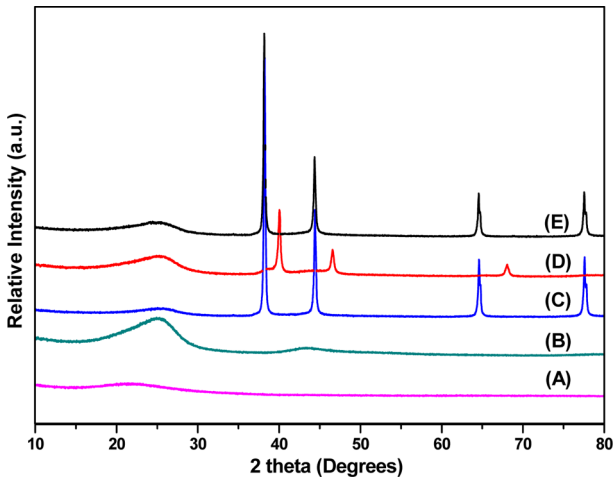

Figure 4. Wide-angle PXRD patterns of NSB-25 (A), CC-25 (B), CGC-25 (C), CPC-25 (D) and CGPC-25 (E).

the diffraction peak of amorphous silica.[5] Two additional peaks, with lower intensity corresponding to graphite-type reflection from the (002) and (100) planes, were observed at 2θ values of 24.9° and 42.9°, respectively, upon switching to CC-25 from NSB-25.[5,6] The XRD of the CGC-25 material showed four additional peaks at 2θ = 38.2°, 44.4, 64.6° and 77.6°, which corresponded to reflections of Au planes (111), (200), (220) and (311) respectively, denoting the formation of noble gold particles with a face centered cubic structure.[7,8] Similarly, the XRD of CPC-25 composite revealed three additional peaks at 2θ = 40.0°, 46.6° and 68.1°, which corresponded to reflections of Pd planes (111), (200), (220), respectively, signifying face-centered cubic structure of palladium. Collective MCNRs composite CGPC-25 shown merged XRD peaks at 2θ = 38.2°, 44.4°, 64.6°, and 77.5°, which corresponded to reflections of Pd-Au plans. All the MCNRs exhibits broad peaks centered at 2θ value of around 20–30° which is consistent with typical amorphous nature of the silica/carbon foundation. The XRD spectra recoded in

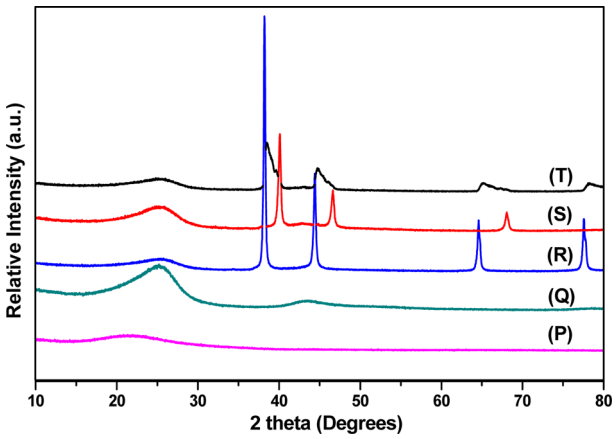

Figure 5. Wide-angle PXRD patterns of NSB-170 (P), CC-170 (Q), CGC-170 (R), CPC-170 (S) and CGPC-170 (T).

the examined area of MCNRs have shown strong signals for both gold and palladium in carbon foundation.

The wide-angle PXRD profile of NSB-170 showed (Figure 5) one broad peak assigned at 2θ = 21.3°, corresponding to the diffraction peak of amorphous silica.[5] Two additional peaks, with lower intensity corresponding to graphite-type reflection from the (002) and (100) planes, were observed at 2θ values of 25.2° and 43.2°, respectively, upon switching to CC-170 from NSB-170.[5,6] The XRD of the CGC-170 material showed four additional peaks at 2θ = 38.2°, 44.4, 64.6° and 77.6°, which corresponded to reflections of Au planes (111), (200), (220) and (311) respectively, denoting the formation of noble gold particles with a face centered cubic structure.[7,8] Similarly, the XRD of CPC-170 composite revealed three additional peaks at 2θ = 40.1°, 46.6° and 68.1°, which corresponded to reflections of Pd planes (111), (200), (220), respectively, signifying face-centered cubic structure of palladium. Collective MCNRs composite CGPC-170 shown combined XRD peaks at 2θ = 38.5°, 39.6°, 44.7°, 46.1°, 65.1°, 68.0° and 78.2°, which corresponded to reflections of Pd-Au plans. All the MCNRs exhibits broad peaks centered at 2θ value of around 20–30° which is consistent with typical amorphous nature of the silica/carbon foundation.

Characterization by SEM Analysis. The structure of the NSB, CC, CGC, CPC and CGPC (25 nm and 170 nm) were investigated by SEM and TEM analysis. The SEM image of NSB-25 (Figure 6A) showed that most particles were uniform, spherical with particle size diameter ~25 nm and closely packed with each other. While SEM images of CC-25 revealed hollow cores of ~25 nm in diameter with interconnected hierarchically porous structure (Figure 6B).[9] They become more regular and smooth after thermal treatment. Additionally, CGC-25, CPC-25 and CGPC-25 showed well stabilized Au, Pd and combined particles on CC-25 with narrow particle diameter, respectively (Figures 6C, 6D and 6E). MCNRs show a clear difference between the carbon cage and the metal (Au, Pd and Au-Pd) nano particles present on the CC-25 backbones. The hierarchically porous composite materials (CC-25) synthesized by the templating approach suggest that the spherical morphology is well-

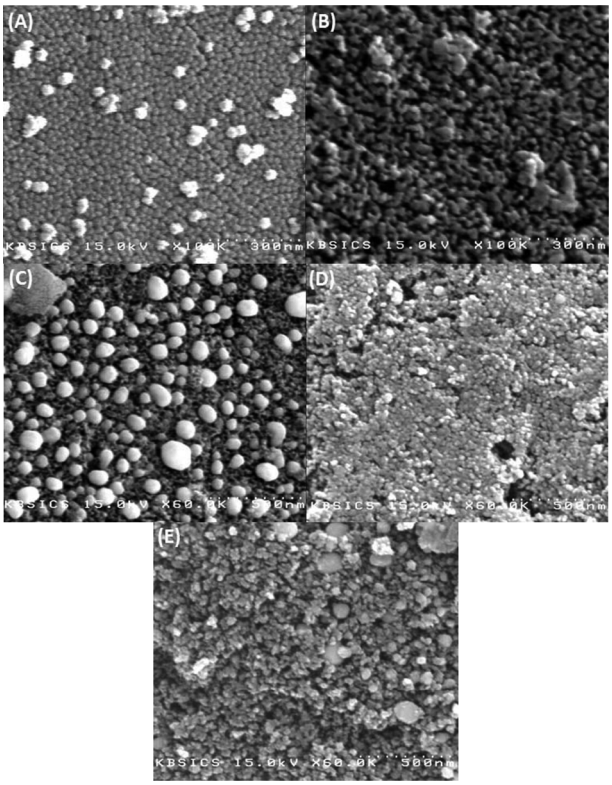

Figure 6. SEM images of NSB-25 (A), CC-25 (B), CGC-25 (C), CPC-25 (D) and CGPC-25 (E).

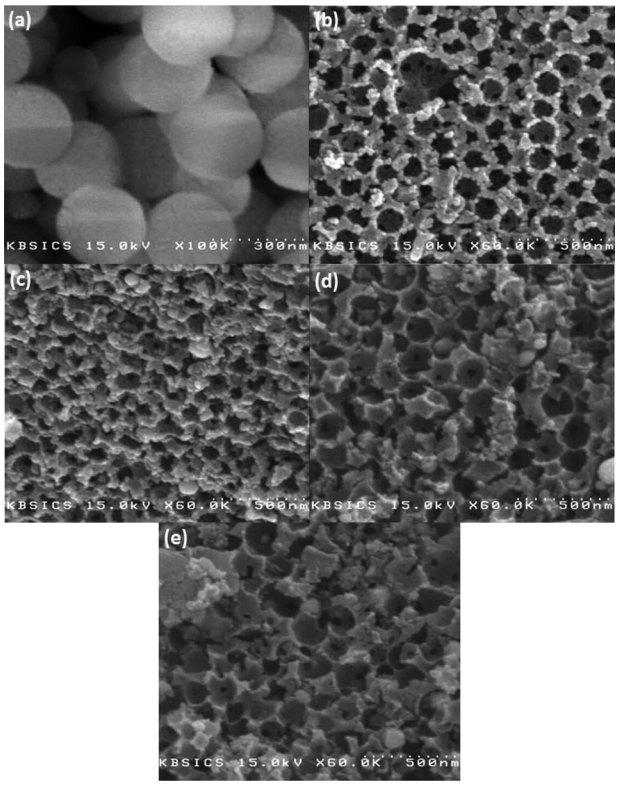

Figure 7. SEM images of NSB-170 (a), CC-170 (b), CGC-170 (c), CPC-170 (d) and CGPC-170 (e).

replicated.

The SEM image of NSB-170 (Figure 7a) showed that most particles were uniform, spherical with particle size diameter ~170 nm and closely packed with each other. While SEM images of CC-170 revealed hollow cores of ~170 nm in diameter with interconnected hierarchically porous struc-

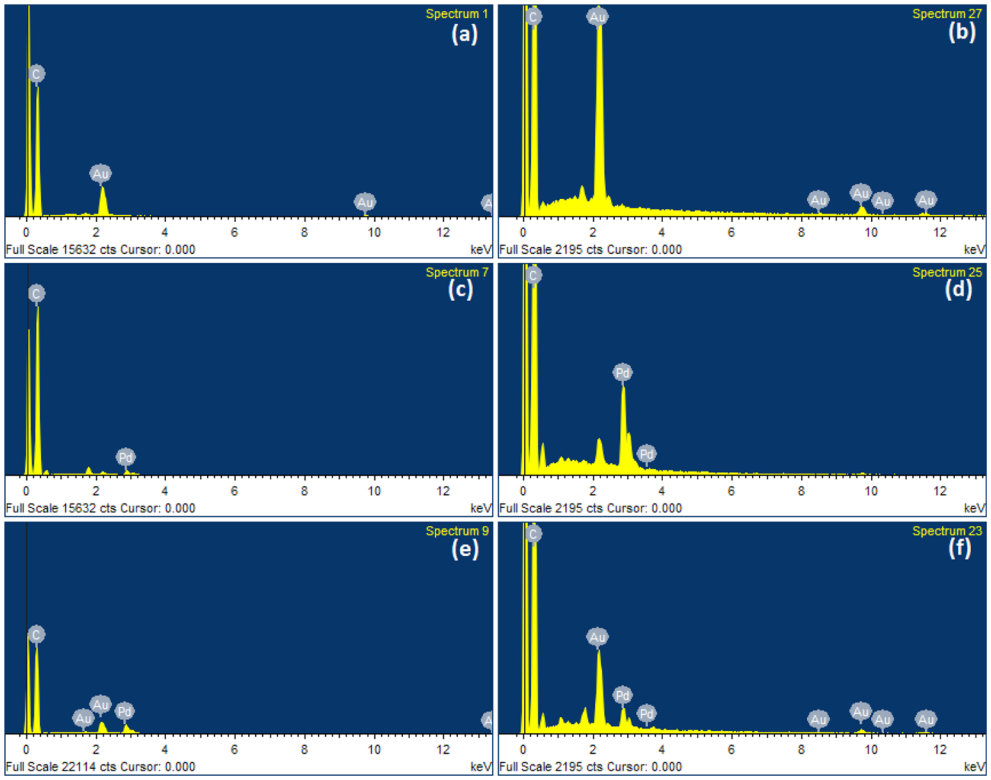

Figure 8. SEM-EDX spectra of CGC-25 (a), CGC-170 (b), CPC-25 (c), CPC-170 (d), CGPC-25 (e) and CGPC-170 (f).

ture (Figure 7b).[9] They become more regular and smooth after thermal treatment. Additionally, CGC-170, CPC-170 and CGPC-170 exhibited well-stabilized Au, Pd and combined particles on CC-170 with little wider particle diameter, respectively. All MCNRs shows a clear difference between the carbon cage and the metal (Au, Pd and Au-Pd) nano particles present on the CC-170 backbones along with replicated hollow and spherical morphology of NSB-170 (Figures 7c, 7d and 7e).

The SEM was coupled with energy dispersive spectroscopy (EDS) to assess the purity and the elemental composition of composite materials (Figure 8). The EDS spectra recoded in the examined area of CGC-25/170, CPC-25/170 and CGPC-25/170 have shown strong signals for gold, palladium and combined along with carbon foundation (Figures 8ab, 8cd, 8ef), respectively. The hierarchically porous MCNRs synthesized by the templating approach suggest that the spherical morphology is well-replicated, too.

Characterization by TEM Analysis. In addition, by comparing the high magnification TEM images of the NSB-25 template (Figure 9A) and replicated composite carbon materials (CC-25) (Figure 9B), it can be observed that the porous structure of the silica template is well imitated. The consistent hollow cores of hierarchically porous CC-25 were identical and strongly connected each other.[9] The TEM image of CGC-25 and CPC-25 confirms that the Au and Pd nanoparticles are homogeneously dispersed and adhere to the carbon cage cores (Figures 9C and 9D). While the TEM image of CGPC-25 shown combined Au and Pd nanoparticles on interconnected hierarchically hollow cores (~25 nm) of carbon structure (Figures 9E and 9F).

Subsequently, by comparing the high magnification TEM images of the NSB-170 template (Figure 10a) and replicated composite carbon materials (CC-170) (Figure 10b), it can be observed that the porous structure of the silica template is well imitated. The consistent hollow cores of hierarchically porous CC-170 were identical and strongly connected each other.[9] The TEM image of CGC-170 and CPC-170 confirms that the Au and Pd nanoparticles are homogeneously dispersed and adhere to the Carbon cage cores (Figures 10c and 10d). While the TEM image of CGPC-170 shown combined Au and Pd nanoparticles on interconnected hierarchically wider hollow cores (~170 nm) of carbon structure (Figures 10e).

Nitrogen Adsorption-desorption Study. The total pore volume of the material was estimated from the amount of N_2

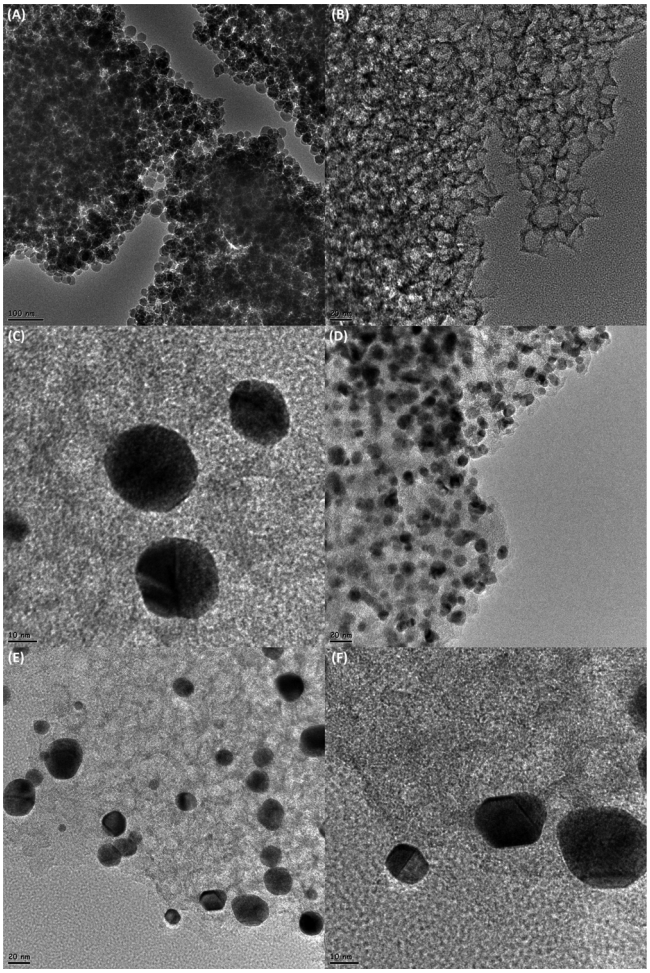

Figure 9. TEM images of NSB-25 (A), CC-25 (B), CGC-25 (C), CPC-25 (D) and CGPC-25 (E and F).

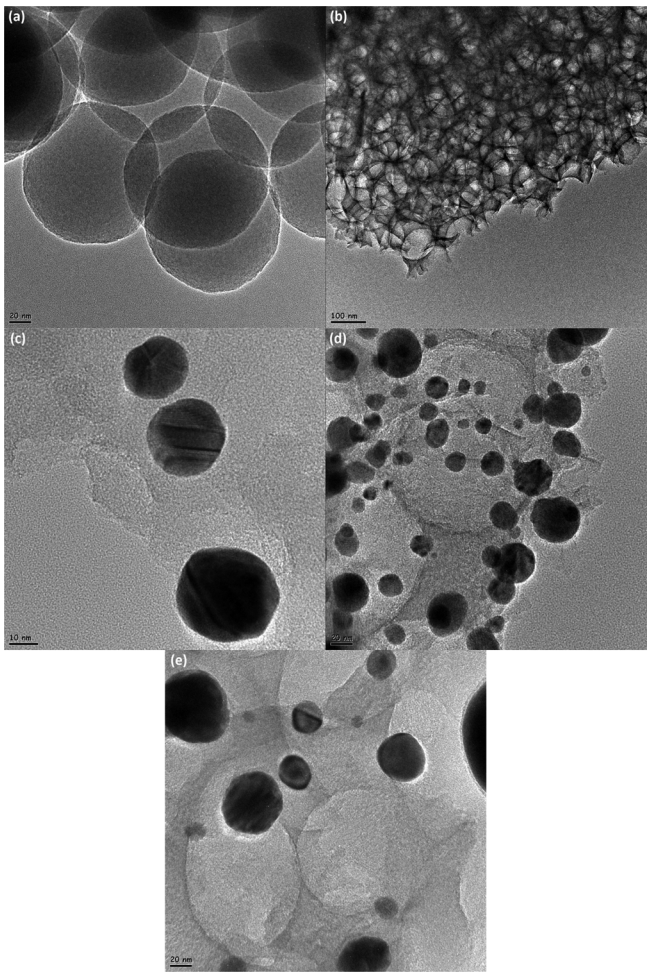

Figure 10. TEM images of NSB-170 (a), CC-170 (b), CGC-170 (c), CPC-170 (d) and CGPC-170 (e).

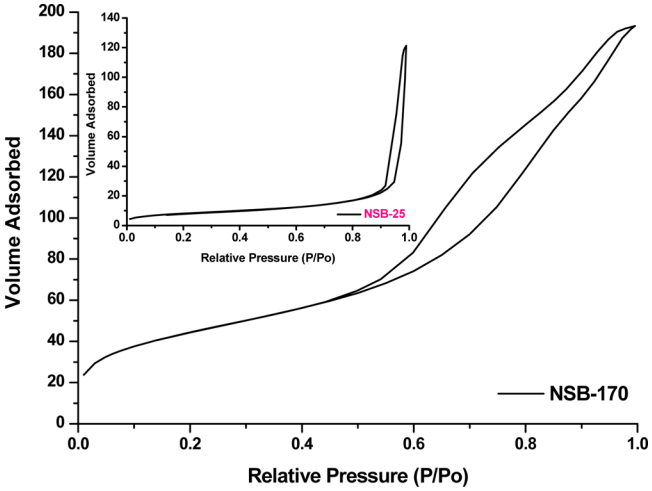

Figure 11. Nitrogen adsorption-desorption isotherms of NSB-25 and NSB-170.

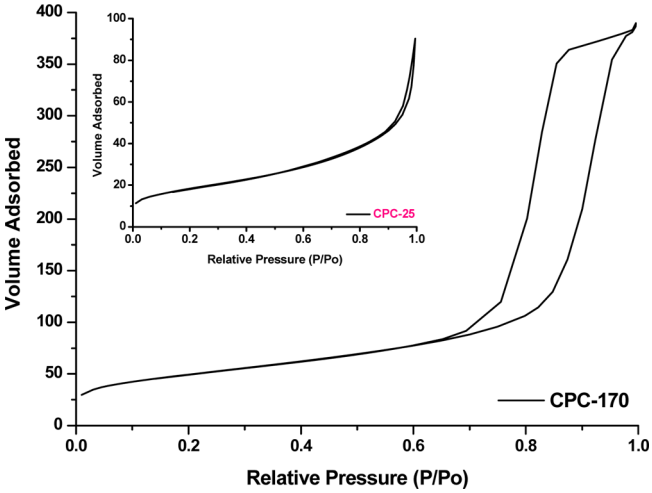

Figure 14. Nitrogen adsorption-desorption isotherms of CPC-25 and CPC-170.

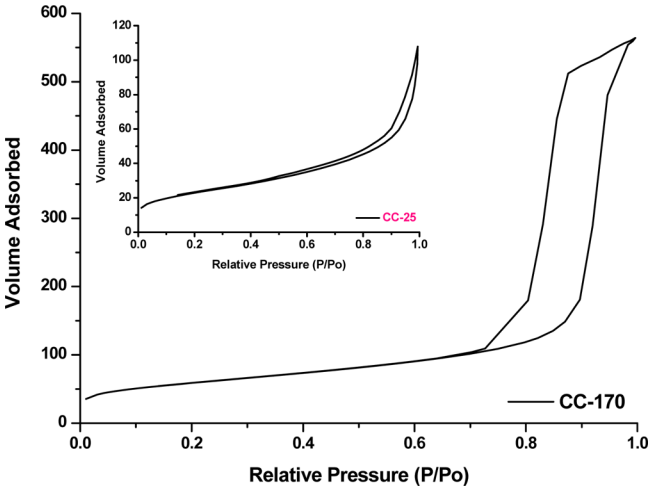

Figure 12. Nitrogen adsorption-desorption isotherms of CC-25 and CC-170.

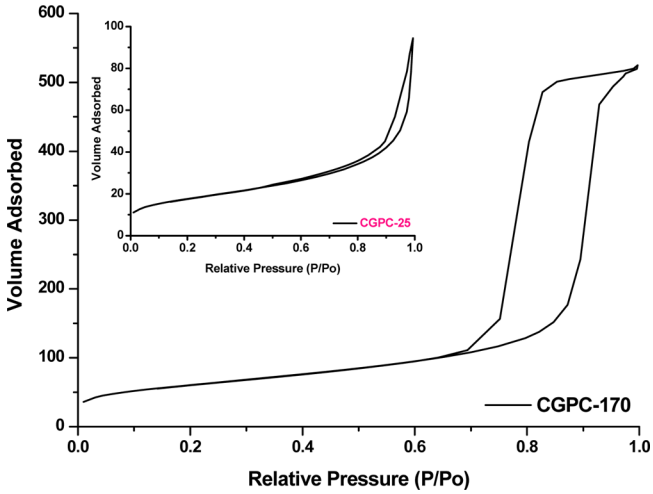

Figure 15. Nitrogen adsorption-desorption isotherms of CGPC-25 and CGPC-170.

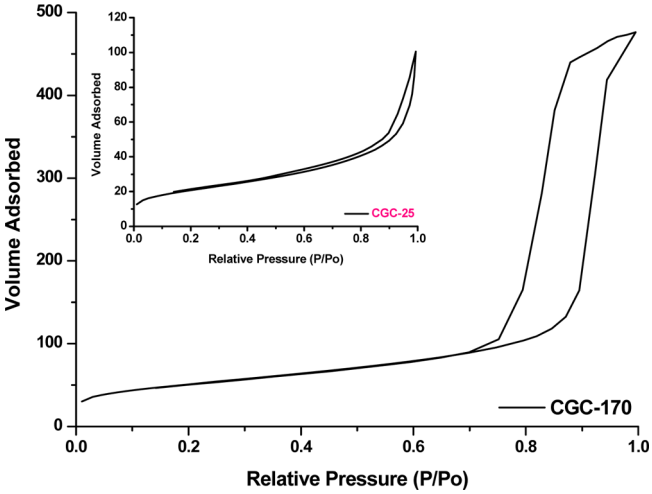

Figure 13. Nitrogen adsorption-desorption isotherms of CGC-25 and CGC-170.

adsorption at relative pressure of about 0.995. The primary mesopore volume *Vp* was calculated from the slope of a linear portion of the *t*-plot in the pressure range above the pressure of nitrogen condensation in primary mesopores. Typical isotherms are shown in Figures 11-15, which represents a pore structure of type *IV* and confirms the well arranged mesopores. The data on BET surface area, BJH pore diameter, total pore volumes found are summarized in Table 1. The NSB-25 gave fair BET surface area (30 m^2/g), total pore volume (0.086 cm^3/g) and 116 Å BJH pore diameter. A large increase in BET surface area was observed (30-82 m^2/g) upon preparation of carbon cage (CC-25). Consequently, reduction in the BJH pore diameter from 116 to 58 Å and tiny rise in total pore volume from 0.086 to 0.120 cm^3/g was observed. On the another hand, small decrease in BET surface area 82 to 75 m^2/g in pore volume from 0.120 to 0.108 cm^3/g and in pore diameter from 58 to 57 Å was observed upon gold incorporation in carbon cage

Table 1. Physico-chemical data of NSB, CC and MCNRs (25 and 170 nm)

Sr. No.	Compound	BET Surface Area (m^2/g)	Total Pore Volume (cm^3/g)	BJH Pore Diameter (Å)	Langmuir Surface Area (m^2/g)
1.	NSB-25	30	0.086	116	38
2.	CC-25	82	0.120	58	105
3.	CGC-25	75	0.108	57	96
4.	CPC-25	66	0.095	58	87
5.	CGPC-25	63	0.092	58	81
6.	NSB-170	163	0.290	71	219
7.	CC-170	212	0.857	162	271
8.	CGC-170	184	0.737	160	246
9.	CPC-170	178	0.584	131	238
10.	CGPC-170	218	0.786	144	292

indicates that the internal pores of the CC-25 are occupied by the gold particles (CGC-25). Similarly, small decrease in BET surface area 82 to 66 m^2/g in pore volume from 0.120 to 0.095 cm^3/g and unchanged pore diameter from 58 to 58 Å was observed upon palladium addition in carbon cage indicates that the internal pores of the CC-25 are occupied by the palladium particles (CPC-25). Moreover, tiny decrease in BET surface area 75 to 63 m^2/g in pore volume from 0.108 to 0.092 cm^3/g and small increment in pore diameter from 57 to 58 Å was observed upon palladium incorporation in CGC-25 indicates that the internal pores of the CGC-25 are occupied by the palladium particles (CGPC-25).

The NSB-170 gave fair BET surface area (163 m^2/g), total pore volume (0.290 cm^3/g) and 71 Å BJH pore diameter. A large increase in BET surface area was observed (163-212 m^2/g) upon preparation of CC-170. Consequently, addition in the BJH pore diameter from 71 to 162 Å and rise in total pore volume from 0.290 to 0.857 cm^3/g was observed. On the another hand, small decrease in BET surface area 212 to 184 m^2/g in pore volume from 0.857 to 0.737 cm^3/g and in pore diameter from 162 to 160 Å was observed upon gold incorporation in CC-170 indicates that the internal pores of the CC-170 are occupied by the gold particles (CGC-170). Similarly, small decrease in BET surface area 212 to 178 m^2/g in pore volume from 0.857 to 0.584 cm^3/g and in pore diameter from 162 to 131 Å was observed upon palladium addition in carbon cage indicates that the internal pores of the CC-170 are occupied by the palladium particles (CPC-170). Moreover, tiny increment in BET surface area 184 to 218 m^2/g in pore volume from 0.737 to 0.786 cm^3/g and small decrease in pore diameter from 160 to 144 Å was observed upon palladium incorporation in CGC-170 indicates that the internal pores of the CGC-170 are occupied by the palladium particles (CGPC-170). The experiment result indicates that the structure of MCNRs are maintained after modification.

Thermal Analysis (TGA/ICP/Elemental analysis). Thermo-gravimetric curves (Figures 16 and 17) shown minor weight losses of about < 10% occurred from 25 to 900 °C for NSB, CC, CGC, CPC and CGPC (25/170 nm). This weight loss can be mainly attributed due to the removal of water molecules and further carbonization between 100-900 °C. Elemental analysis data of CC-25 indicate that carboni-

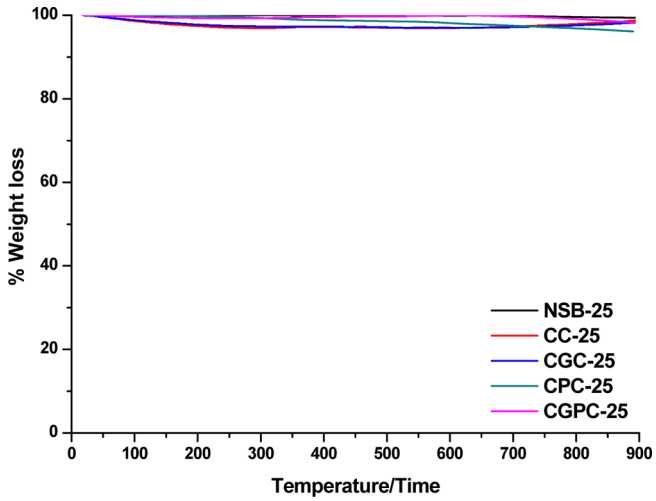

Figure 16. Thermo-gravimetric analysis (TGA) curves of NSB-25, CC-25, CGC-25, CPC-25 and CGPC-25.

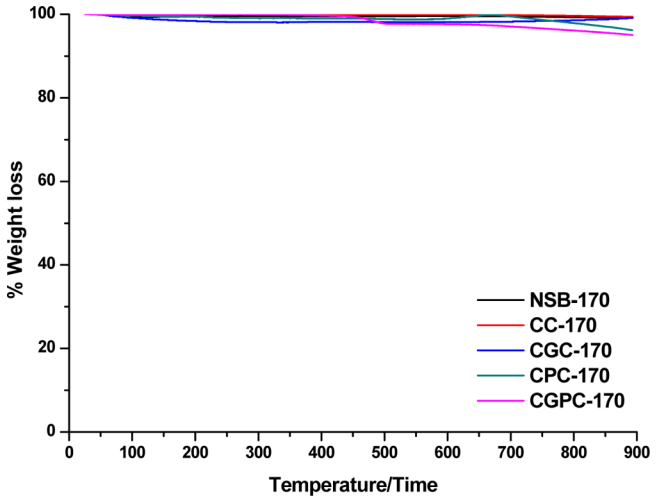

Figure 17. Thermo-gravimetric analysis (TGA) curves of NSB-170, CC-170, CGC-170, CPC-170 and CGPC-170.

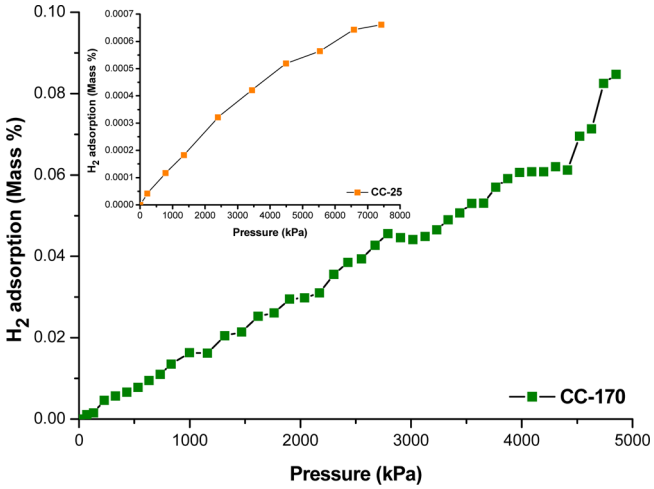

Figure 18. Hydrogen adsorption isotherms of CC-25 and CC-170.

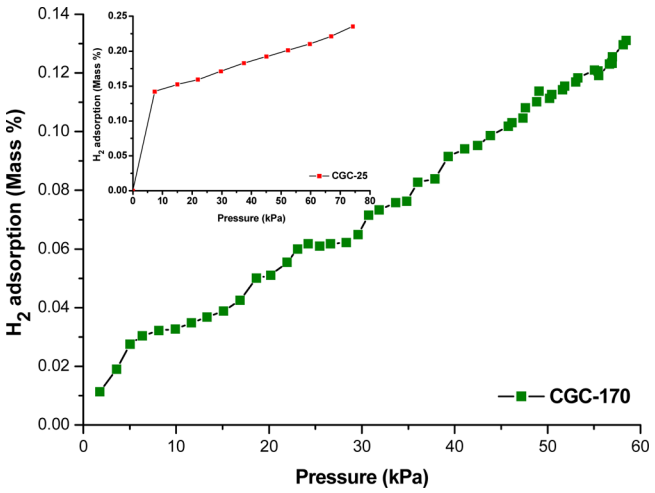

Figure 19. Hydrogen adsorption isotherms of CGC-25 and CGC-170.

zation (> 900 °C) is almost completely achieved, with < 6% oxygen and hydrogen remaining, respectively, thus suggesting that a pure carbon, homologous framework is obtained. ICP analysis of CGC-25 and CPC-25 showed 11.0 wt % and 2.3 wt % gold and palladium metals respectively. ICP measurement of CGPC-25 revealed 9.1 wt % and 6.8 wt % combined gold and palladium metals which is required to be present to make carbon gold palladium composite material (CGPC-25).

Elemental analysis data of CC-170 indicate that carbonization (> 900 °C) is almost completely achieved, with < 5% oxygen and hydrogen remaining, respectively, thus suggesting that a pure carbon, homologous framework is obtained. ICP analysis of CGC-170 and CPC-170 showed 10.2 wt % and 3.4 wt % gold and palladium metals respectively. ICP measurement of CGPC-170 revealed 4.5 wt % and 2.9 wt % combined gold and palladium metals which is required to be present to make carbon gold palladium composite material (CGPC-170).

Hydrogen Adsorption Study. The hydrogen adsorption isotherms were performed by using gravimetric measurement with a Rubotherm MSB in four steps: blank measurement, loading and reactivation of samples, buoyancy measurement and adsorption measurement. The adsorption measurement at 25 °C was done up to 80 bar pressure. The samples were activated in situ by controlled heating up to 400 °C (heating rage 1 °C/min) under high vacuum and the temperature and vacuum were maintained for 12 h before sorption measurements. The amount of activated adsorbent was determined from the weight of the absorbent before as well as after activation and prior to start of adsorption measurement. After activation, the samples were allowed to cool down to the desired temperature and the temperature was maintained during entire analysis using external water circulator. Hydrogen with a specific pressure steps was introduced into the sample chamber. The increase weight of the sample due to hydrogen adsorption was accurately measured using MSB connected to the sample holder. Typically, 0.2–0.7 g of samples were used in experiment. Adsorption isotherms of CC-25, CC-170, CGC-25 and CGC-170 were conducted in order to evaluate the enhancement of the modified carbons. The hydrogen adsorption capacity of all compounds are expressed in terms of wt % (weight of the hydrogen molecules/weight of the material × 100).

The adsorption of hydrogen in pristine CC-25, CC-170, CGC-25 and CGC-170 were investigated using static gravimetric adsorption system. The experimental hydrogen uptake capacities at 25 °C up to 80 bar pressure for CC-25/170 and CGC-25/170 are shown in Figures 18 and 19. The adsorption of hydrogen took place in a potential region which restrained the hydrogen adsorption domain. The hydrogen adsorption of CGC-25 and CGC-170 showed a maximum hydrogen adsorption capacity of 0.13 wt % (58.5 kPa) and 0.24 wt % (74.2 kPa), respectively. The adsorption capacity of CGC-25/170 increased with increasing pressure at room temperature. On the other hand, hydrogen adsorption was absent for pristine CC-25 and CC-170 at pressures up to 8000 kPa and 5000 kPa, respectively. In general, the experimental results illustrate that the hydrogen adsorption ability of the MCNRs (CGC-25/170) was greatly improved compared to that of the non-metal CC-25 and CC-170 base, in terms of percentage mass uptake per unit pressure. It was found that gold-deposited MCNRs can lead to higher hydrogen storage compare to pristine carbon cage (CC-25/170) as a result of weak chemisorptions process initiated by the so-called “spillover” effect.

References

1. Mayani, S. V.; Mayani, V. J.; Park, S. K.; Kim, S. W. *Mater. Lett.* **2012**, *82*, 120.
2. Mayani, V. J.; Mayani, S. V.; Lee, Y.; Park, S. K. *Sep. Purif. Technol.* **2011**, *80*, 90.
3. Mayani, V. J.; Mayani, S. V.; Kim, S. W. *Mater. Lett.* **2012**, *87*, 90.
4. Perrin, D. D.; Armarego, W. L. F.; Perrin, D. R. *Purification of Laboratory Chemicals*; Pergamon, New York: 1981.
5. Guo, X.; Liu, X.; Xu, B.; Dou, T. *Colloids Surf., A* **2009**, *345*, 141.
6. Kao, L. H.; Hsu, T. C. *Mater. Lett.* **2008**, *62*, 695.

7. Vermisoglou, E. C.; Romanos, G. E.; Tzitzios, V.; Karanikolos, G. N.; Akylas, V.; Delimitis, A.; Pilatos, G.; Kanellopoulos, N. K. *Microporous Mesoporous Mater.* **2009**, *120*, 122.
8. Yang, G. W.; Gao, G. Y.; Wang, C.; Xu, C.-L.; Li, H. –L. *Carbon* **2008**, *46*, 747.
9. Li, Q.; Jiang, R.; Dou, Y.; Wu, Z.; Huang, T.; Feng, D.; Yang, J.; Yu, A.; Zhao, D. *Carbon* **2011**, *49*, 1248.